EUROPEAN ORGANIZATION FOR NUCLEAR RESEARCH

CERN-EP/99-137
September 29, 1999

Searches for Scalar Quarks in e^+e^- Interactions at $\sqrt{s} = 189$ GeV

The L3 Collaboration

Abstract

Searches for scalar top and scalar bottom quarks, as well as for mass-degenerate scalar quarks of the first two families are performed at 189 GeV centre-of-mass energy with the L3 detector at LEP. No signals are observed. Model-independent limits on the scalar top production cross sections are determined for the decay modes $\tilde{t}_1 \to c\tilde{\chi}^0_1$ and $\tilde{t}_1 \to b\ell\tilde{\nu}$. For scalar quarks of the other flavours $\tilde{q} \to q\tilde{\chi}^0_1$ decays are considered. Within the framework of the Minimal Supersymmetric Standard Model mass limits are set at 95% C.L. for these particles. Indirect limits on the gluino mass are also derived.

Submitted to *Phys. Lett. B*

1 Introduction

In the Minimal Supersymmetric extension of the Standard Model (MSSM) [1] for each helicity state of Standard Model (SM) quarks, $\mathrm{q_{L,R}}$, there is a corresponding scalar SUSY partner $\mathrm{\tilde{q}_{L,R}}$. Generally, the left, $\mathrm{\tilde{q}_L}$, and right, $\mathrm{\tilde{q}_R}$, eigenstates mix to form mass eigenstates. The mixing is proportional to the corresponding SM quark mass and to the parameter $a_\mathrm{q} = A_\mathrm{q} - \mu \cot\beta$ for up type quarks and $a_\mathrm{q} = A_\mathrm{q} - \mu \tan\beta$ for down type ones. A_q is the trilinear coupling among scalars, μ the Higgsino mass parameter and $\tan\beta$ the ratio of the vacuum expectation values of the two Higgs fields. For the first two generations of scalar quarks (squarks) the weak eigenstates are also mass eigenstates to a good approximation. However, this does not hold for the squarks of the third family. Due to the heavy top quark the $\mathrm{\tilde{t}_L} - \mathrm{\tilde{t}_R}$ mixing is enhanced, leading to a large splitting between the two mass eigenstates. This is usually expressed in terms of the mixing angle, θ_LR. The lighter scalar top (stop) quark

$$\mathrm{\tilde{t}_1} = \mathrm{\tilde{t}_L} \cos\theta_\mathrm{LR} + \mathrm{\tilde{t}_R} \sin\theta_\mathrm{LR} \quad (1)$$

can thus be well within the discovery range of LEP. Furthermore, if $\tan\beta \gtrsim 10$, large $\mathrm{\tilde{b}_L} - \mathrm{\tilde{b}_R}$ mixing occurs. This may lead to a scalar bottom (sbottom) quark, $\mathrm{\tilde{b}_1}$, also light enough to be accessible at LEP.

In the present analysis, R-parity conservation is assumed, which implies that SUSY particles (sparticles) are produced in pairs; heavier sparticles decay into lighter ones and the Lightest Supersymmetric Particle (LSP) is stable. In the MSSM the best LSP candidate is the weakly interacting lightest neutralino, $\tilde{\chi}^0_1$.

Squark pair production at LEP proceeds via the exchange of Z/γ bosons in the s-channel. The production cross section is governed by two free parameters: the squark mass and the mixing angle, θ_LR [2]. At $\cos\theta_\mathrm{LR} \sim 0.57$ the stop decouples from the Z and the cross section is minimal. The corresponding value is $\cos\theta_\mathrm{LR} \sim 0.39$ for the sbottom. The cross section reaches the maximum at $\cos\theta_\mathrm{LR}$=1 when the light squark mass eigenstate is the weak eigenstate.

At LEP energies the most important stop decay channels are: $\mathrm{\tilde{t}_1} \rightarrow \mathrm{c}\tilde{\chi}^0_1$, $\mathrm{b}\nu_\ell\tilde{\ell}$, $\mathrm{b}\ell\tilde{\nu}_\ell$, and $\mathrm{b}\tilde{\chi}^+_1$, where the $\tilde{\ell}$ and $\tilde{\nu}_\ell$ are the supersymmetric partners of the charged leptons and neutrinos, and the $\tilde{\chi}^0_1$ and $\tilde{\chi}^+_1$ are the lightest neutralino and chargino, respectively. The $\mathrm{\tilde{t}_1} \rightarrow \mathrm{b}\tilde{\chi}^\pm_1$ decay channel is the dominant one when kinematically allowed. However, the current limits on the chargino mass [3] preclude this decay to occur, except for a small region in the MSSM parameter space with the common scalar mass (m_0) from 60 to 90 GeV. Similarly, the $\mathrm{\tilde{t}_1} \rightarrow \mathrm{b}\nu_\ell\tilde{\ell}$ decay is precluded by the current limits [4] on charged scalar lepton masses. The stop analysis is performed considering the $\mathrm{\tilde{t}_1} \rightarrow \mathrm{c}\tilde{\chi}^0_1$ and $\mathrm{\tilde{t}_1} \rightarrow \mathrm{b}\ell\tilde{\nu}_\ell$ decay channels, with $\tilde{\nu}_\ell$ decaying invisibly $\tilde{\nu}_\ell \rightarrow \nu_\ell\tilde{\chi}^0_1$. Since the $\mathrm{\tilde{t}_1} \rightarrow \mathrm{c}\tilde{\chi}^0_1$ is a flavour changing weak decay, the $\mathrm{\tilde{t}_1} \rightarrow \mathrm{b}\ell\tilde{\nu}_\ell$ channel is dominant when kinematically allowed. Therefore the two decay modes are investigated each with the assumption of 100% branching fraction. For the stop three-body decay channel $\mathrm{\tilde{t}_1} \rightarrow \mathrm{b}\ell\tilde{\nu}_\ell$, two scenarios are considered: ℓ being e, μ or τ with equal probabilities or pure τ. The latter occurs at high $\tan\beta$ values.

For sbottom, as well as for the first two generations of squarks, the $\mathrm{\tilde{q}} \rightarrow \mathrm{q}\tilde{\chi}^0_1$ decay mode is investigated under the assumption of 100% branching fraction.

Since the stop two-body decay $\mathrm{\tilde{t}_1} \rightarrow \mathrm{c}\tilde{\chi}^0_1$ is a second order weak decay, the lifetime of the $\mathrm{\tilde{t}_1}$ is larger than the typical hadronisation time of 10^{-23}s. The $\mathrm{\tilde{t}_1} \rightarrow \mathrm{b}\ell\tilde{\nu}$ decay proceeds via a virtual chargino exchange and the lifetime is also expected to be larger than the hadronisation time. Thus the stop will first hadronise and then decay. For the sbottom the situation depends on the gaugino-higgsino content of the neutralino: for a gaugino-like neutralino the sbottom lifetime is expected to be larger than the hadronisation time. In the present analysis a 'hadronisation before decay' scenario is followed. Although hadronisation does not change the final event topology, it affects the track multiplicity, the jet properties and the event shape.

The present study supersedes previous L3 limits on stop and sbottom quark productions [5]. Searches for supersymmetric quarks have been performed by other LEP [6] and by TEVATRON [7, 8] experiments.

2 Data Samples and Simulation

The data used in the present analysis were collected in 1998 at $\sqrt{s}$=189 GeV using the L3 detector [9]. The total integrated luminosity is 176.4 pb^{-1}.

Monte Carlo (MC) samples of squark events are generated using a PYTHIA based event generator [10]. The squark mass has been varied from 45 GeV up to the kinematical limit and the $\tilde{\chi}_1^0$ mass from 1 GeV to $M_{\tilde{t}_1}-2$ GeV or to $M_{\tilde{b}_1}-5$ GeV for the stop and sbottom two-body decay modes. The $\tilde{t}_1 \rightarrow b\ell\tilde{\nu}$ and $\tilde{t}_1 \rightarrow b\tau\tilde{\nu}$ channels are generated with $\tilde{\nu}$ mass from 43 GeV to $M_{\tilde{t}_1} - 7$ GeV. In total 160 samples are generated, each with at least 2000 events.

The following MC programs are used to estimate the Standard Model backgrounds: PYTHIA [11] for $e^+e^- \rightarrow q\bar{q}$, $e^+e^- \rightarrow ZZ$ and $e^+e^- \rightarrow Ze^+e^-$, KORALZ [12] for $e^+e^- \rightarrow \tau^+\tau^-$, KORALW [13] for $e^+e^- \rightarrow W^+W^-$, EXCALIBUR [14] for $e^+e^- \rightarrow W^\pm e^\mp \nu$, PHOJET [15] for $e^+e^- \rightarrow e^+e^-q\bar{q}$ and DIAG36 [16] for $e^+e^- \rightarrow e^+e^-\tau^+\tau^-$. The number of simulated events for each background process exceeds by 100 times the statistics of the collected data samples except for the two-photon collision processes, for which the MC statistics amounts to only twice the data.

The response of the L3 detector is simulated using the GEANT 3.15 package [17]. It takes into account effects of energy loss, multiple scattering and showering in the detector materials and in the beam pipe. Hadronic interactions are simulated with the GHEISHA program [18].

3 Event Preselection

The signal events of $\tilde{t}_1 \rightarrow c\tilde{\chi}_1^0$ and $\tilde{b}_1 \rightarrow b\tilde{\chi}_1^0$ contain two high multiplicity acoplanar jets originated from c or b-quarks. In addition, two charged leptons are present in the $\tilde{t}_1 \rightarrow b\ell\tilde{\nu}$ decay channel. The neutralinos and sneutrinos in the final state escape detection leading to missing energy in the event. A common preselection is applied to obtain a sample of unbalanced hadronic events. The events have to fulfil the following requirements: more than four tracks; at least 10 but not more than 40 calorimetric clusters; a visible energy, E_{vis}, between 5 GeV and 150 GeV; an energy deposition in the forward calorimeters less than 10 GeV and a total energy in the 30° cone around the beam pipe less than $0.25\times E_{\mathrm{vis}}$; a transverse missing momentum, $P_{\mathrm{T}}^{\mathrm{miss}}$, greater than 2 GeV and a sinus of the polar angle of the missing momentum, $\sin\theta_{\mathrm{miss}}$, greater than 0.2.

After the preselection 3110 events are retained, compared with 3514 ± 48 expected from the SM processes, which are dominated by two-photon interactions. Figure 1 shows the distributions of E_{vis}; the absolute value of the total momentum of the two jets projected onto the direction perpendicular to the thrust axis computed in the transverse plane, E_{TTJ}; the energy of the most energetic lepton, E_ℓ and the b-tagging event discriminant, D_{Btag}. D_{Btag} is defined as the negative log-likelihood of the probability for the event to be consistent with light quark production [19]. After preselection the data and MC are in good agreement. The discrepancy in the total number of data and MC events is localised in the low E_{vis} region, which is dominated by two-photon processes. This effect is taken into account by assigning a systematic error of 10–20% on the two-photon cross section.

4 Selection Optimisation

The kinematics of the signal events strongly depend on the mass difference between squark and neutralino, $\Delta M = M_{\tilde{\mathrm{q}}} - M_{\tilde{\chi}^0_1}$. In the very low ΔM region, the visible energy and track multiplicity are low. Therefore, signal events are difficult to separate from the two-photon interactions. For high ΔM values, signal events will be similar to $\mathrm{W^+W^-}$, $\mathrm{W^\pm e^\mp \nu}$ or ZZ final states. The most favourable region for the signal and background separation is expected at ΔM=20–40 GeV.

To cope with the various background sources, the searches are performed independently in different ΔM regions. For $\tilde{\mathrm{t}}_1 \rightarrow \mathrm{c}\tilde{\chi}^0_1$ and $\tilde{\mathrm{b}}_1 \rightarrow \mathrm{b}\tilde{\chi}^0_1$ decays four selections have been optimised. These selections typically cover ΔM regions of: 5–10 GeV, 10–20 GeV, 20–40 GeV and $\gtrsim 40$ GeV. In case of $\tilde{\mathrm{t}}_1 \rightarrow \mathrm{b}\ell\tilde{\nu}$ decays three selections are devised for each lepton flavour. These selections cover the $\Delta M = M_{\tilde{\mathrm{q}}} - M_{\tilde{\nu}}$ region consistent with the limit $M_{\tilde{\nu}} \gtrsim 43$ GeV from LEP1 [20].

The following kinematic variables are used in the selections: Lower cuts on E_{vis}, $P_{\mathrm{T}}^{\mathrm{miss}}$ and $P_{\mathrm{T}}^{\mathrm{miss}}/E_{\mathrm{vis}}$ separate signal from two-photon background, whereas an upper cut on E_{vis} removes $\mathrm{W^+W^-}$, $\mathrm{W^\pm e^\mp \nu}$, ZZ and $\mathrm{Ze^+e^-}$ events. A cut on $\sin\theta_{\mathrm{miss}}$ rejects $\mathrm{e^+e^-q\bar{q}}$ events. Cuts on jet acollinearity and acoplanarity reduce the $\mathrm{q\bar{q}}$ contribution. A veto on the energy deposition in the 50° azimuthal sector around the missing momentum direction suppresses $\tau^+\tau^-$ and $\mathrm{q\bar{q}}$ events. The $\mathrm{W^+W^-}$ production, where one W decays leptonically and $\mathrm{W^\pm e^\mp \nu}$ events are removed by vetoing energetic isolated leptons. The cut on E_{TTJ} suppresses $\mathrm{e^+e^-q\bar{q}}$, $\mathrm{q\bar{q}}$ as well as $\mathrm{W^+W^-}$ backgrounds.

For the selections of $\tilde{\mathrm{b}}_1 \rightarrow \mathrm{b}\tilde{\chi}^0_1$ and $\tilde{\mathrm{t}}_1 \rightarrow \mathrm{b}\ell\tilde{\nu}$ signal events, cuts are applied on the event b-tagging variable D_{Btag}.

At least one isolated lepton is required in the case of $\tilde{\mathrm{t}}_1 \rightarrow \mathrm{b}\ell\tilde{\nu}$ decays. An electron is isolated if the calorimetric energy deposition in a 10° cone around its direction is less than 2 GeV. Muon isolation requirement implies an energy deposition in the cone between 5° to 10° around its direction of less than 2 GeV. A tau is isolated when the calorimetric energy deposition in the cone between 10° to 20° around its direction is less than 2 GeV and less than 50% of the tau energy. Furthermore, the energy deposition in a cone between 20° to 30° must be less than 60% of the tau energy. Finally, a lower cut on the energy of the most energetic lepton in the event is applied in order to suppress mainly the two-photon and the $\mathrm{q\bar{q}}$ backgrounds.

The cut values on the kinematic variables are chosen by an optimisation procedure for the different ΔM regions. The procedure minimises the average limit for an infinite number of trials assuming only background contributions [21]. For each signal mass point, the optimal selection or combination of selections is chosen.

The expected signal efficiencies for a 90 GeV stop and sbottom at various ΔM values are given in Table 1 together with the SM background expectations.

5 Systematic Errors

The errors arising from the signal MC statistics vary from 3% to 8% for the stop and from 3% to 7% for the sbottom depending on selection efficiencies.

The main systematic errors on the signal selection efficiency arise from the uncertainties in the squark production, hadronisation and decay scheme. We have studied the following sources of systematic errors:

- The squark signals are generated assuming $\cos\theta_{\mathrm{LR}}$=1. However, as their coupling to the Z depends on $\cos\theta_{\mathrm{LR}}$, the initial state radiation spectrum is also mixing angle dependent. The maximal influence of this source has been evaluated by generating signal samples with the values of $\cos\theta_{\mathrm{LR}}$ when the squarks decouple from the Z. The largest decrease in the selection efficiencies, 4% for stop and 6% for sbottom, is observed at low $\Delta M \sim$ 5–10 GeV. With increasing ΔM the selection efficiencies are less affected by this source of systematics. At $\Delta M \sim 70$ GeV the error is estimated to be negligible. Conservatively, for the limit calculation we use the efficiencies obtained at decoupling values of $\cos\theta_{\mathrm{LR}}$.

- The invariant mass available for spectator quarks has been assumed to be M_{eff}=0.5 GeV [22]. The hadronic energy and track multiplicity of the event depend on the value of this variable. A variation of M_{eff} from 0.25 GeV to 0.75 GeV [22] results in $4-12\%$ relative change in efficiency for stop and $6-8\%$ for sbottom.

- For the hadron containing a squark, the Peterson fragmentation scheme [23] is used with the parameter $\epsilon_{\tilde{\mathrm{q}}}$ propagated from ϵ_{b} such that $\epsilon_{\tilde{\mathrm{q}}} = \epsilon_{\mathrm{b}} m_{\mathrm{b}}^2/m_{\tilde{\mathrm{q}}}^2$ with $\epsilon_{\mathrm{b}} = 0.0035$ [24] and m_{b}=5 GeV. The ϵ_{b} is varied in the range from 0.002 to 0.006 [24]. This induces $5-12\%$ and $2-6\%$ changes in the selection efficiencies for $\tilde{\mathrm{t}}_1$ and $\tilde{\mathrm{b}}_1$, respectively.

- For the $\tilde{\mathrm{t}}_1 \rightarrow \mathrm{c}\tilde{\chi}_1^0$ decays the uncertainty on the c-quark fragmentation parameter ϵ_{c} results in a $1-4\%$ change in efficiency when ϵ_{c} is varied from 0.02 to 0.06 [24]. The central value is chosen to be $\epsilon_{\mathrm{c}} = 0.03$ [24].

- For the stop three-body decay mode $\tilde{\mathrm{t}}_1 \rightarrow \mathrm{b}\ell\tilde{\nu}$, the weak structure of the decay matrix element [25] is taken into account. The related possible source of systematics has been evaluated by generating signal events with only a phase-space model. The selection efficiencies are slightly higher in this case. Therefore the efficiency values obtained with the matrix element are used.

The overall relative systematic error on the selection efficiencies ranges from 7% to 16% and from 7% to 11% for stop and sbottom, respectively. This error and the uncertainty on the background normalisation, dominated by MC statistics, as well as the quoted uncertainty on two-photon background, are incorporated [26] in the final results.

6 Results

Table 2 summarises the number of selected data and expected background events with different ΔM selections for all investigated channels. A total of 35 and 18 candidates appear in the $\tilde{\mathrm{t}}_1 \rightarrow \mathrm{c}\tilde{\chi}_1^0$ and $\tilde{\mathrm{b}}_1 \rightarrow \mathrm{b}\tilde{\chi}_1^0$ selections, whereas 33.1 ± 4.3 and 13.5 ± 3.3 are expected from the SM processes. The numbers of $\tilde{\mathrm{t}}_1 \rightarrow \mathrm{b}\ell\tilde{\nu}$ and $\tilde{\mathrm{t}}_1 \rightarrow \mathrm{b}\tau\tilde{\nu}$ candidates are 9 and 18, compared with 11.3 ± 3.0 and 21.4 ± 4.4 expected events.

The composition of the expected background into two-fermion, four-fermion and two-photon processes is given in Table 3. When all the ΔM selections for all investigated channels are applied, 59 events are retained. This is consistent with 60.4 $\pm$ 6.5 events expected from SM processes, mainly due to two-photon interactions. Thus no evidence for stop or sbottom is found and upper limits are derived on their production cross sections.

Model-independent cross section limits in the $M_{\tilde{\mathrm{q}}}$, $M_{\tilde{\chi}^0_1}$ plane are given in Figure 2 for stop and sbottom assuming 100% branching fraction for the $\tilde{\mathrm{t}}_1 \rightarrow \mathrm{c}\tilde{\chi}^0_1$ and $\tilde{\mathrm{b}}_1 \rightarrow \mathrm{b}\tilde{\chi}^0_1$ decays. The limits are obtained by combining the present results with those obtained at $\sqrt{s} = 161 - 172$ GeV and 183 GeV [5]. The evaluated limits correspond to luminosity weighted average cross sections. In the medium ΔM region cross sections larger than 0.08 pb are excluded.

The cross section limits for stop production assuming $\tilde{\mathrm{t}}_1 \rightarrow \mathrm{b}\ell\tilde{\nu}$ decay, in the two scenarios for lepton flavours, ℓ=e, μ, τ with equal probability or ℓ=τ, are given in Figure 3. Cross sections larger than 0.05 pb are excluded if the mass difference $\Delta M = M_{\tilde{\mathrm{q}}} - M_{\tilde{\nu}}$ is greater than $25 - 35$ GeV.

7 MSSM Interpretation

In the MSSM the stop and sbottom production cross sections depend on the squark mass and the mixing angle $\cos\theta_{\mathrm{LR}}$. Comparing the theoretical prediction with the 95% C.L. limit on the production cross section, we determine the excluded mass regions for $\tilde{\mathrm{t}}_1$ and $\tilde{\mathrm{b}}_1$. Figure 4a shows the excluded $\tilde{\mathrm{t}}_1$ mass region as a function of $M_{\tilde{\mathrm{t}}_1}$ and $M_{\tilde{\chi}^0_1}$ at $\cos\theta_{\mathrm{LR}}$=1 and 0.57 for the $\tilde{\mathrm{t}}_1 \rightarrow \mathrm{c}\tilde{\chi}^0_1$ decay. For this decay mode, stop masses below 88 GeV are excluded under the assumptions of ΔM=$M_{\tilde{\mathrm{t}}_1} - M_{\tilde{\chi}^0_1}$ greater than 15 GeV and $\cos\theta_{\mathrm{LR}}$=1. For the same values of ΔM and in the most pessimistic scenario of $\cos\theta_{\mathrm{LR}}$=0.57, the mass limit is 81 GeV. The region where $\tilde{\mathrm{t}}_1 \rightarrow \mathrm{bW}\tilde{\chi}^0_1$ decay is kinematically accessible and becoming the dominant decay mode, is also indicated. This decay is not considered in the analysis.

The exclusion plot for the sbottom is given in Figure 4b for $\cos\theta_{\mathrm{LR}}$=1 and $\cos\theta_{\mathrm{LR}}$=0.39. Sbottom masses below 85 GeV are excluded assuming ΔM greater than 15 GeV and $\cos\theta_{\mathrm{LR}}$=1. In the most pessimistic scenario of $\cos\theta_{\mathrm{LR}}$=0.39, the mass limit obtained is 64 GeV.

The excluded stop mass regions, if the dominant three-body decays are kinematically open, are given in Figure 5. Figure 5a corresponds to $\tilde{\mathrm{t}}_1 \rightarrow \mathrm{b}\ell\tilde{\nu}$, ℓ=e, μ, τ with equal probability. Here the lower $\tilde{\mathrm{t}}_1$ mass limits are 89 GeV and 86 GeV for $\cos\theta_{\mathrm{LR}}$=1 and 0.57, respectively. The corresponding exclusion limits for stop decays through $\tilde{\mathrm{t}}_1 \rightarrow \mathrm{b}\tau\tilde{\nu}$ are shown in Figure 5b. Mass limits of 88 GeV and 83 GeV are obtained, assuming ΔM >15 GeV.

For a fixed value of ΔM =15 GeV the excluded stop and sbottom masses as a function of the mixing angle are shown in Figure 6. The exclusion limits mainly reflect the cross section behaviour. At $\cos\theta_{\mathrm{LR}}$=1, the $\tilde{\mathrm{t}}_1$ and $\tilde{\mathrm{b}}_1$ cross sections are quite similar. As $\cos\theta_{\mathrm{LR}}$ decreases squark production proceeds mainly via γ exchange rendering the sbottom production cross section about 4 times lower than that of the stop. Consequently, the sbottom exclusion limits are relatively modest at low $\cos\theta_{\mathrm{LR}}$ values.

For squarks of the first two generations, the same selection efficiencies are assumed as for the stop two-body decays, because of the similar event topologies (jets and missing energy). Then the cross section limits given in Figure 2a are interpreted in terms of degenerate squark masses. Figure 7a shows the squark mass limit as a function of the LSP mass. Two scenarios are considered: “left” and “right” squark degeneracy or only “right” squark production. In the first case, with four degenerate squark flavours, the mass limit is set at 91.5 GeV for ΔM

greater than 10 GeV. In the case of only “right” squark production, the mass limit is 90 GeV. The regions excluded, if all squarks but the stop are degenerate are also shown.

Assuming gaugino unification at the GUT scale, the results on the four degenerate squarks are reinterpreted on the $M_{\tilde{\mathrm{g}}}$, $M_{\tilde{\mathrm{q}}}$ plane as shown in Figure 7b. Moreover, the gaugino unification allows a transformation of the absolute limit on M_2, obtained from the chargino, neutralino and scalar lepton searches [3], into a limit on the gluino mass as shown in Figure 7b. This is done using the ISAJET program [27]. For $\tan\beta = 4$, gluino masses up to about 210−250 GeV are excluded at 95% C.L.

Acknowledgements

We thank S. Kraml for many useful discussions and comments. We wish to express our gratitude to the CERN accelerator division for the excellent performance of the LEP machine. We acknowledge the effort of those engineers and technicians who have participated in the construction and maintenance of this experiment.

References

[1] For a review see, *e.g.* H.E. Haber and G.L. Kane, Phys. Rep. **117** (1985) 75.

[2] A. Bartl *et al.*, Z.Phys **C 73** (1997) 469.

[3] L3 Collab., M. Acciarri *et al.*, *Search for charginos and Neutralinos in* e^+e^- *collisions at* $\sqrt{s}$*=189 GeV*, contributed paper n. 7-46 to *EPS-HEP99*, Tampere, July 1999, and also submitted to Phys. Lett.

[4] L3 Collab., M. Acciarri *et al.*, *Search for Scalar leptons in* e^+e^- *collisions at* $\sqrt{s}$*=189 GeV*, contributed paper n. 7-46 to *EPS-HEP99*, Tampere, July 1999, and also submitted to Phys. Lett.

[5] L3 Collaboration, M. Acciarri *et al.*, Phys. Lett. **B 445** (1999) 428.

[6] ALEPH Collaboration, R. Barate *et al.*, Phys. Lett. **B 434** (1998) 189;
DELPHI Collaboration, P. Abreu *et al.*, Eur. Phys. J. **C 6** (1999) 385;
OPAL Collaboration, G. Abbiendi *et al.*, Phys. Lett. **B 456** (1999) 95.

[7] Ch. Holck for the CDF Collaboration, hep-ex/9903060.

[8] The D0 Collaboration, S. Abachi *et al.*, Phys. Rev. Lett. **76** (1996) 2222;
D. Hedin for the D0 Collaboration, FERMILAB-Conf-99/047-E.

[9] The L3 Collaboration, B. Adeva *et al.*, Nucl. Instr. and Meth. **A 289** (1990) 35;
M. Chemarin *et al.*, Nucl. Instr. and Meth. **A 349** (1994) 345;
M. Acciarri *et al.*, Nucl. Instr. and Meth. **A 351** (1994) 300;
G. Basti *et al.*, Nucl. Instr. and Meth. **A 374** (1996) 293;
I.C. Brock *et al.*, Nucl. Instr. and Meth. **A 381** (1996) 236;
A. Adam *et al.*, Nucl. Instr. and Meth. **A 383** (1996) 342.

[10] Modified version of OPAL MC generator for squarks production, E. Accomodo *et al.*,, 'Physics at LEP2', eds. G. Altarelli, T. Sjöstrand and F. Zwirner, CERN 96-01, vol. 2, 286; paper in preparation..

[11] T. Sjöstrand, `PYTHIA 5.7` and `JETSET 7.4` Physics and Manual, CERN-TH/7112/93 (1993), revised August 1995; Comp. Phys. Comm. **82** (1994) 74.

[12] S. Jardach, B.F.L. Ward, and Z. Wąs, Comp. Phys. Comm. **79** (1994) 503.
Version 4.02 was used.

[13] M. Skrzypek *et al.*, Comp. Phys. Comm. **94** (1996) 216;
M. Skrzypek *et al.*, Phys. Lett. **B 372** (1996) 289.
Version 1.21 was used.

[14] F.A. Berends, R. Kleiss, and R. Pittau, Nucl. Phys. **B 424** (1994) 308; Nucl. Phys. **B 426** (1994) 344; Nucl. Phys. (Proc. Suppl.) **B 37** (1994) 163; Phys. Lett. **B 335** (1994) 490; Comp. Phys. Comm. **85** (1995) 447.

[15] R. Engel, Z. Phys. **C 66** (1995) 203; R. Engel and J. Ranft, Phys. Rev. **D 54** (1996) 4244.
Version 1.05 was used.

[16] F.A. Berends, P.H. Daverfeldt and R. Kleiss, Nucl. Phys. **B 253** (1985) 441.

[17] R. Brun *et al.*, CERN DD/EE/84-1 (Revised 1987).

[18] H. Fesefeldt, RWTH Aachen Report PITHA 85/2 (1985).

[19] L3 Collaboration, M. Acciarri *et al.*, Phys. Lett. **B 411** (1997) 373..

[20] C. Caso *et al.*, Eur. Phys. J. **C 3** (1998) 1.

[21] J.F. Grivaz and F. Le Diberder, preprint LAL-92-37, June 1992.

[22] D.S. Hwang, C.S. Kim and W. Namgung, Preprint hep-ph/9412377;
V. Barger, C.S. Kim and R.J.N. Phillips, Preprint MAD/PH/501, 1989.

[23] C. Peterson *et al.*, Phys. Rev. **D 27** (1983) 105.

[24] The LEP Experiments: ALEPH, DELPHI, L3, OPAL, Nucl. Instr. and Meth. **A 378** (1996) 101.

[25] K. Hikasa and M. Kobayashi, Phys. Rev. **D 36** (1987) 724.

[26] R.D. Cousins and V.L. Highland, Nucl. Inst. Meth. **A 320** (1992) 331.

[27] H. Baer *et al.*, in Proceedings of the Workshop on Physics at Current Accelerators and Supercolliders, ed. J. Hewett and D. Zeppenfeld (Argonne National Laboratory, Argonne, Illinois, 1993).

[28] CDF Collaboration, F. Abe *et al.*, Phys. Rev. **D 56** (1997) 1357;
D0 Collaboration, S. Abachi *et al.*, Phys. Rev. Lett. **75** (1995) 618..

[29] UA1 Collaboration, C. Albajar *et al.*, Phys. Lett. **B 198** (1987) 261;
UA2 Collaboration, J. Alitti *et al.*, Phys. Lett. **B 235** (1990) 363.

The L3 Collaboration:

M.Acciarri,[26] P.Achard,[19] O.Adriani,[16] M.Aguilar-Benitez,[25] J.Alcaraz,[25] G.Alemanni,[22] J.Allaby,[17] A.Aloisio,[28] M.G.Alviggi,[28] G.Ambrosi,[19] H.Anderhub,[47] V.P.Andreev,[6,36] T.Angelescu,[12] F.Anselmo,[9] A.Arefiev,[27] T.Azemoon,[3] T.Aziz,[10] P.Bagnaia,[35] L.Baksay,[42] A.Balandras,[4] R.C.Ball,[3] S.Banerjee,[10] Sw.Banerjee,[10] A.Barczyk,[47,45] R.Barillère,[17] L.Barone,[35] P.Bartalini,[22] M.Basile,[9] R.Battiston,[32] A.Bay,[22] F.Becattini,[16] U.Becker,[14] F.Behner,[47] L.Bellucci,[16] J.Berdugo,[25] P.Berges,[14] B.Bertucci,[32] B.L.Betev,[47] S.Bhattacharya,[10] M.Biasini,[32] A.Biland,[47] J.J.Blaising,[4] S.C.Blyth,[33] G.J.Bobbink,[2] A.Böhm,[1] L.Boldizsar,[13] B.Borgia,[35] D.Bourilkov,[47] M.Bourquin,[19] S.Braccini,[19] J.G.Branson,[38] V.Brigljevic,[47] F.Brochu,[4] A.Buffini,[16] A.Buijs,[43] J.D.Burger,[14] W.J.Burger,[32] J.Busenitz,[42] A.Button,[3] X.D.Cai,[14] M.Campanelli,[47] M.Capell,[14] G.Cara Romeo,[9] G.Carlino,[28] A.M.Cartacci,[16] J.Casaus,[25] G.Castellini,[16] F.Cavallari,[35] N.Cavallo,[28] C.Cecchi,[19] M.Cerrada,[25] F.Cesaroni,[23] M.Chamizo,[19] Y.H.Chang,[49] U.K.Chaturvedi,[18] M.Chemarin,[24] A.Chen,[49] G.Chen,[7] G.M.Chen,[7] H.F.Chen,[20] H.S.Chen,[7] X.Chereau,[4] G.Chiefari,[28] L.Cifarelli,[37] F.Cindolo,[9] C.Civinini,[16] I.Clare,[14] R.Clare,[14] G.Coignet,[4] A.P.Colijn,[2] N.Colino,[25] S.Costantini,[8] F.Cotorobai,[12] B.Cozzoni,[9] B.de la Cruz,[25] A.Csilling,[13] S.Cucciarelli,[32] T.S.Dai,[14] J.A.van Dalen,[30] R.D'Alessandro,[16] R.de Asmundis,[28] P.Déglon,[19] A.Degré,[4] K.Deiters,[45] D.della Volpe,[28] P.Denes,[34] F.DeNotaristefani,[35] A.De Salvo,[47] M.Diemoz,[35] D.van Dierendonck,[2] F.Di Lodovico,[47] C.Dionisi,[35] M.Dittmar,[47] A.Dominguez,[38] A.Doria,[28] M.T.Dova,[18,♯] D.Duchesneau,[4] D.Dufournaud,[4] P.Duinker,[2] I.Duran,[39] H.El Mamouni,[24] A.Engler,[33] F.J.Eppling,[14] F.C.Erné,[2] P.Extermann,[19] M.Fabre,[45] R.Faccini,[35] M.A.Falagan,[25] S.Falciano,[35,17] A.Favara,[17] J.Fay,[24] O.Fedin,[36] M.Felcini,[47] T.Ferguson,[33] F.Ferroni,[35] H.Fesefeldt,[1] E.Fiandrini,[32] J.H.Field,[19] F.Filthaut,[17] P.H.Fisher,[14] I.Fisk,[38] G.Forconi,[14] L.Fredj,[19] K.Freudenreich,[47] C.Furetta,[26] Yu.Galaktionov,[27,14] S.N.Ganguli,[10] P.Garcia-Abia,[5] M.Gataullin,[31] S.S.Gau,[11] S.Gentile,[35,17] N.Gheordanescu,[12] S.Giagu,[35] Z.F.Gong,[20] G.Grenier,[24] O.Grimm,[47] M.W.Gruenewald,[8] M.Guida,[37] R.van Gulik,[2] V.K.Gupta,[34] A.Gurtu,[10] L.J.Gutay,[44] D.Haas,[5] A.Hasan,[29] D.Hatzifotiadou,[9] T.Hebbeker,[8] A.Hervé,[17] P.Hidas,[13] J.Hirschfelder,[33] H.Hofer,[47] G. Holzner,[47] H.Hoorani,[33] S.R.Hou,[49] I.Iashvili,[46] B.N.Jin,[7] L.W.Jones,[3] P.de Jong,[2] I.Josa-Mutuberría,[25] R.A.Khan,[18] D.Kamrad,[46] M.Kaur,[18,◇] M.N.Kienzle-Focacci,[19] D.Kim,[35] D.H.Kim,[41] J.K.Kim,[41] S.C.Kim,[41] J.Kirkby,[17] D.Kiss,[13] W.Kittel,[30] A.Klimentov,[14,27] A.C.König,[30] A.Kopp,[46] I.Korolko,[27] V.Koutsenko,[14,27] M.Kräber,[47] R.W.Kraemer,[33] W.Krenz,[1] A.Kunin,[14,27] P.Ladron de Guevara,[25] I.Laktineh,[24] G.Landi,[16] K.Lassila-Perini,[47] P.Laurikainen,[21] A.Lavorato,[37] M.Lebeau,[17] A.Lebedev,[14] P.Lebrun,[24] P.Lecomte,[47] P.Lecoq,[17] P.Le Coultre,[47] H.J.Lee,[8] J.M.Le Goff,[17] R.Leiste,[46] E.Leonardi,[35] P.Levtchenko,[36] C.Li,[20] C.H.Lin,[49] W.T.Lin,[49] F.L.Linde,[2] L.Lista,[28] Z.A.Liu,[7] W.Lohmann,[46] E.Longo,[35] Y.S.Lu,[7] K.Lübelsmeyer,[1] C.Luci,[17,35] D.Luckey,[14] L.Lugnier,[24] L.Luminari,[35] W.Lustermann,[47] W.G.Ma,[20] M.Maity,[10] L.Malgeri,[17] A.Malinin,[27,17] C.Maña,[25] D.Mangeol,[30] P.Marchesini,[47] G.Marian,[15] J.P.Martin,[24] F.Marzano,[35] G.G.G.Massaro,[2] K.Mazumdar,[10] R.R.McNeil,[6] S.Mele,[17] L.Merola,[28] M.Meschini,[16] W.J.Metzger,[30] M.von der Mey,[1] A.Mihul,[12] H.Milcent,[17] G.Mirabelli,[35] J.Mnich,[17] G.B.Mohanty,[10] P.Molnar,[8] B.Monteleoni,[16,†] T.Moulik,[10] G.S.Muanza,[24] F.Muheim,[19] A.J.M.Muijs,[2] M.Musy,[35] M.Napolitano,[28] F.Nessi-Tedaldi,[47] H.Newman,[31] T.Niessen,[1] A.Nisati,[35] H.Nowak,[46] Y.D.Oh,[41] G.Organtini,[35] R.Ostonen,[21] C.Palomares,[25] D.Pandoulas,[1] S.Paoletti,[35,17] P.Paolucci,[28] R.Paramatti,[35] H.K.Park,[33] I.H.Park,[41] G.Pascale,[35] G.Passaleva,[17] S.Patricelli,[28] T.Paul,[11] M.Pauluzzi,[32] C.Paus,[17] F.Pauss,[47] D.Peach,[17] M.Pedace,[35] S.Pensotti,[26] D.Perret-Gallix,[4] B.Petersen,[30] D.Piccolo,[28] F.Pierella,[9] M.Pieri,[16] P.A.Piroué,[34] E.Pistolesi,[26] V.Plyaskin,[27] M.Pohl,[47] V.Pojidaev,[27,16] H.Postema,[14] J.Pothier,[17] N.Produit,[19] D.O.Prokofiev,[44] D.Prokofiev,[36] J.Quartieri,[37] G.Rahal-Callot,[47,17] M.A.Rahaman,[10] P.Raics,[15] N.Raja,[10] R.Ramelli,[47] P.G.Rancoita,[26] G.Raven,[38] P.Razis,[29] D.Ren,[47] M.Rescigno,[35] S.Reucroft,[11] T.van Rhee,[43] S.Riemann,[46] K.Riles,[3] A.Robohm,[47] J.Rodin,[42] B.P.Roe,[3] L.Romero,[25] A.Rosca,[8] S.Rosier-Lees,[4] J.A.Rubio,[17] D.Ruschmeier,[8] H.Rykaczewski,[47] S.Saremi,[6] S.Sarkar,[35] J.Salicio,[17] E.Sanchez,[17] M.P.Sanders,[30] M.E.Sarakinos,[21] C.Schäfer,[1] V.Schegelsky,[36] S.Schmidt-Kaerst,[1] D.Schmitz,[1] H.Schopper,[48] D.J.Schotanus,[30] G.Schwering,[1] C.Sciacca,[28] D.Sciarrino,[19] A.Seganti,[9] L.Servoli,[32] S.Shevchenko,[31] N.Shivarov,[40] V.Shoutko,[27] E.Shumilov,[27] A.Shvorob,[31] T.Siedenburg,[1] D.Son,[41] B.Smith,[33] P.Spillantini,[16] M.Steuer,[14] D.P.Stickland,[34] A.Stone,[6] H.Stone,[34,†] B.Stoyanov,[40] A.Straessner,[1] K.Sudhakar,[10] G.Sultanov,[18] L.Z.Sun,[20] H.Suter,[47] J.D.Swain,[18] Z.Szillasi,[42,¶] T.Sztaricskai,[42,¶] X.W.Tang,[7] L.Tauscher,[5] L.Taylor,[11] C.Timmermans,[30] Samuel C.C.Ting,[14] S.M.Ting,[14] S.C.Tonwar,[10] J.Tóth,[13] C.Tully,[34] K.L.Tung,[7] Y.Uchida,[14] J.Ulbricht,[47] E.Valente,[35] G.Vesztergombi,[13] I.Vetlitsky,[27] D.Vicinanza,[37] G.Viertel,[47] S.Villa,[11] M.Vivargent,[4] S.Vlachos,[5] I.Vodopianov,[36] H.Vogel,[33] H.Vogt,[46] I.Vorobiev,[27] A.A.Vorobyov,[36] A.Vorvolakos,[29] M.Wadhwa,[5] W.Wallraff,[1] M.Wang,[14] X.L.Wang,[20] Z.M.Wang,[20] A.Weber,[1] M.Weber,[1] P.Wienemann,[1] H.Wilkens,[30] S.X.Wu,[14] S.Wynhoff,[1] L.Xia,[31] Z.Z.Xu,[20] B.Z.Yang,[20] C.G.Yang,[7] H.J.Yang,[7] M.Yang,[7] J.B.Ye,[20] S.C.Yeh,[50] An.Zalite,[36] Yu.Zalite,[36] Z.P.Zhang,[20] G.Y.Zhu,[7] R.Y.Zhu,[31] A.Zichichi,[9,17,18] F.Ziegler,[46] G.Zilizi,[42,¶] M.Zöller.[1]

1 I. Physikalisches Institut, RWTH, D-52056 Aachen, FRG[§]
III. Physikalisches Institut, RWTH, D-52056 Aachen, FRG[§]
2 National Institute for High Energy Physics, NIKHEF, and University of Amsterdam, NL-1009 DB Amsterdam, The Netherlands
3 University of Michigan, Ann Arbor, MI 48109, USA
4 Laboratoire d'Annecy-le-Vieux de Physique des Particules, LAPP,IN2P3-CNRS, BP 110, F-74941 Annecy-le-Vieux CEDEX, France
5 Institute of Physics, University of Basel, CH-4056 Basel, Switzerland
6 Louisiana State University, Baton Rouge, LA 70803, USA
7 Institute of High Energy Physics, IHEP, 100039 Beijing, China[△]
8 Humboldt University, D-10099 Berlin, FRG[§]
9 University of Bologna and INFN-Sezione di Bologna, I-40126 Bologna, Italy
10 Tata Institute of Fundamental Research, Bombay 400 005, India
11 Northeastern University, Boston, MA 02115, USA
12 Institute of Atomic Physics and University of Bucharest, R-76900 Bucharest, Romania
13 Central Research Institute for Physics of the Hungarian Academy of Sciences, H-1525 Budapest 114, Hungary[‡]
14 Massachusetts Institute of Technology, Cambridge, MA 02139, USA
15 Lajos Kossuth University-ATOMKI, H-4010 Debrecen, Hungary[¶]
16 INFN Sezione di Firenze and University of Florence, I-50125 Florence, Italy
17 European Laboratory for Particle Physics, CERN, CH-1211 Geneva 23, Switzerland
18 World Laboratory, FBLJA Project, CH-1211 Geneva 23, Switzerland
19 University of Geneva, CH-1211 Geneva 4, Switzerland
20 Chinese University of Science and Technology, USTC, Hefei, Anhui 230 029, China[△]
21 SEFT, Research Institute for High Energy Physics, P.O. Box 9, SF-00014 Helsinki, Finland
22 University of Lausanne, CH-1015 Lausanne, Switzerland
23 INFN-Sezione di Lecce and Universitá Degli Studi di Lecce, I-73100 Lecce, Italy
24 Institut de Physique Nucléaire de Lyon, IN2P3-CNRS,Université Claude Bernard, F-69622 Villeurbanne, France
25 Centro de Investigaciones Energéticas, Medioambientales y Tecnologícas, CIEMAT, E-28040 Madrid, Spain♭
26 INFN-Sezione di Milano, I-20133 Milan, Italy
27 Institute of Theoretical and Experimental Physics, ITEP, Moscow, Russia
28 INFN-Sezione di Napoli and University of Naples, I-80125 Naples, Italy
29 Department of Natural Sciences, University of Cyprus, Nicosia, Cyprus
30 University of Nijmegen and NIKHEF, NL-6525 ED Nijmegen, The Netherlands
31 California Institute of Technology, Pasadena, CA 91125, USA
32 INFN-Sezione di Perugia and Universitá Degli Studi di Perugia, I-06100 Perugia, Italy
33 Carnegie Mellon University, Pittsburgh, PA 15213, USA
34 Princeton University, Princeton, NJ 08544, USA
35 INFN-Sezione di Roma and University of Rome, "La Sapienza", I-00185 Rome, Italy
36 Nuclear Physics Institute, St. Petersburg, Russia
37 University and INFN, Salerno, I-84100 Salerno, Italy
38 University of California, San Diego, CA 92093, USA
39 Dept. de Fisica de Particulas Elementales, Univ. de Santiago, E-15706 Santiago de Compostela, Spain
40 Bulgarian Academy of Sciences, Central Lab. of Mechatronics and Instrumentation, BU-1113 Sofia, Bulgaria
41 Center for High Energy Physics, Adv. Inst. of Sciences and Technology, 305-701 Taejon, Republic of Korea
42 University of Alabama, Tuscaloosa, AL 35486, USA
43 Utrecht University and NIKHEF, NL-3584 CB Utrecht, The Netherlands
44 Purdue University, West Lafayette, IN 47907, USA
45 Paul Scherrer Institut, PSI, CH-5232 Villigen, Switzerland
46 DESY, D-15738 Zeuthen, FRG
47 Eidgenössische Technische Hochschule, ETH Zürich, CH-8093 Zürich, Switzerland
48 University of Hamburg, D-22761 Hamburg, FRG
49 National Central University, Chung-Li, Taiwan, China
50 Department of Physics, National Tsing Hua University, Taiwan, China
§ Supported by the German Bundesministerium für Bildung, Wissenschaft, Forschung und Technologie
‡ Supported by the Hungarian OTKA fund under contract numbers T019181, F023259 and T024011.
¶ Also supported by the Hungarian OTKA fund under contract numbers T22238 and T026178.
♭ Supported also by the Comisión Interministerial de Ciencia y Tecnología.
♯ Also supported by CONICET and Universidad Nacional de La Plata, CC 67, 1900 La Plata, Argentina.
◇ Also supported by Panjab University, Chandigarh-160014, India.
△ Supported by the National Natural Science Foundation of China.
† Deceased.

Table 1: Selection efficiencies, ϵ, and number of expected events from SM processes, N_{SM}, for a 90 GeV stop and sbottom, as a function of ΔM (see text).

ΔM (GeV)	$\tilde{t}_1 \to c\tilde{\chi}^0_1$		$\tilde{t}_1 \to b\ell\tilde{\nu}$		$\tilde{t}_1 \to b\tau\tilde{\nu}$		$\tilde{b}_1 \to b\tilde{\chi}^0_1$	
	ϵ (%)	N_{SM}	ϵ (%)	N_{SM}	ϵ (%)	N_{SM}	ϵ (%)	N_{SM}
2	0.1	17.7	-	-	-	-	-	-
5	17.5	17.7	-	-	-	-	0.06	12.3
7	21.6	21.8	15.8	10.7	5.6	12.3	17.6	12.3
10	19.1	4.10	39.5	10.7	14.0	12.3	14.5	12.7
20	48.1	7.80	57.3	2.30	41.5	8.50	35.4	0.46
30	62.7	4.37	45.3	0.59	35.2	1.58	42.8	0.73
40	39.5	4.37	46.0	0.59	39.3	1.58	34.0	1.19
47	47.0	11.9	37.1	0.59	35.2	1.58	29.7	1.19
60	44.3	11.9	-	-	-	-	22.8	0.52
80	38.4	7.54	-	-	-	-	23.0	0.52
88	38.0	7.54	-	-	-	-	21.6	0.52

Table 2: Number of observed events, N_{D}, and SM background expectations, N_{SM}, for the stop and sbottom selections at very low (5–10 GeV), low (10–20 GeV), medium (20–40 GeV) and high ($\gtrsim$ 40 GeV) ΔM. The quoted errors are due to MC statistics only.

Selection	$\tilde{\mathrm{t}}_1 \to \mathrm{c}\tilde{\chi}^0_1$		$\tilde{\mathrm{t}}_1 \to \mathrm{b}\ell\tilde{\nu}$		$\tilde{\mathrm{t}}_1 \to \mathrm{b}\tau\tilde{\nu}$		$\tilde{\mathrm{b}}_1 \to \mathrm{b}\tilde{\chi}^0_1$	
	N_{D}	N_{SM}	N_{D}	N_{SM}	N_{D}	N_{SM}	N_{D}	N_{SM}
Very low ΔM	19	17.7 ± 4.0	7	8.4 ± 2.7	14	12.3 ± 3.4	16	12.3 ± 3.3
Low ΔM	3	4.1 ± 1.4	2	2.3 ± 1.3	4	8.5 ± 2.7	0	0.46 ± 0.22
Medium ΔM	5	4.37 ± 0.63	0	0.59 ± 0.15	0	1.58 ± 0.94	1	0.72 ± 0.26
High ΔM	8	7.54 ± 0.74	-	-	-	-	2	0.52 ± 0.14
Combined	35	33.1 ± 4.3	9	11.3 ± 3.0	18	21.4 ± 4.4	18	13.5 ± 3.3

Table 3: Number of observed events, N_{D}, and SM background expectations, N_{SM}, for the stop and sbottom selections. The contribution of two-fermion ($\mathrm{q\bar{q}}$, $\tau^+\tau^-$), four-fermion ($\mathrm{W^+W^-}$, $\mathrm{W^\pm e^\mp}\nu$, ZZ, $\mathrm{Ze^+e^-}$) and two-photon ($\mathrm{e^+e^-q\bar{q}}$, $\mathrm{e^+e^-}\tau^+\tau^-$) processes are given separately. The quoted errors are due to MC statistics only.

Channel	N_{D}	$N_{\mathrm{two-fermion}}$	$N_{\mathrm{four-fermion}}$	$N_{\mathrm{two-photon}}$	N_{SM}
$\tilde{\mathrm{t}}_1 \to \mathrm{c}\tilde{\chi}^0_1$	35	0.41 ± 0.16	13.6 ± 1.1	19.1 ± 4.2	33.1 ± 4.3
$\tilde{\mathrm{t}}_1 \to \mathrm{b}\ell\tilde{\nu}$	9	0.29 ± 0.15	0.97 ± 0.24	10.0 ± 3.0	11.3 ± 3.0
$\tilde{\mathrm{t}}_1 \to \mathrm{b}\tau\tilde{\nu}$	18	0.29 ± 0.15	0.49 ± 0.19	20.5 ± 4.4	21.4 ± 4.4
$\tilde{\mathrm{b}}_1 \to \mathrm{b}\tilde{\chi}^0_1$	18	0.17 ± 0.12	1.45 ± 0.35	11.8 ± 3.3	13.5 ± 3.3
Total	59	0.84 ± 0.25	14.5 ± 1.1	45.1 ± 6.5	60.4 ± 6.5

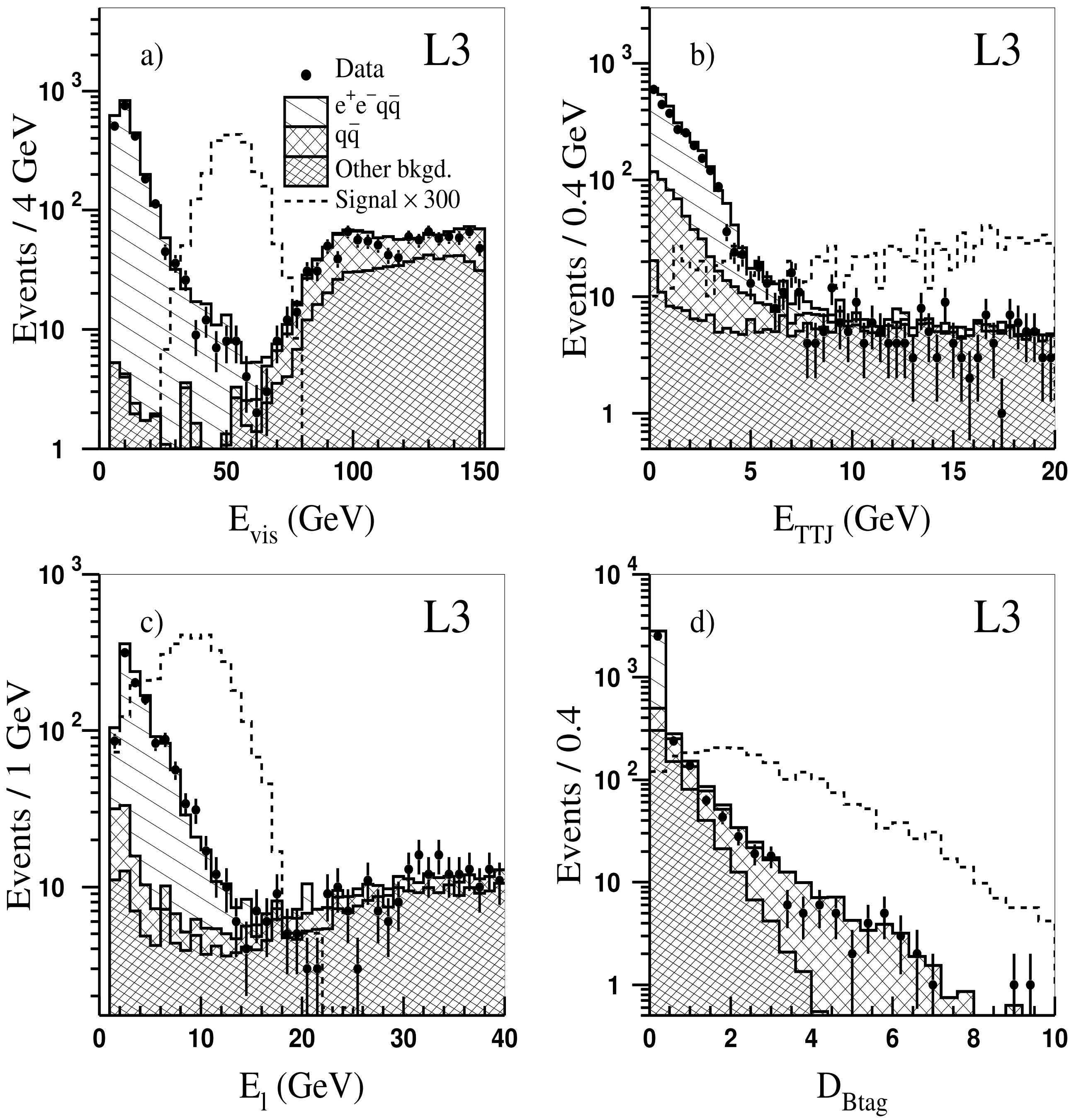

Figure 1: Distributions of a) E_{vis}, b) E_{TTJ} (see text), c) the most energetic lepton energy E_ℓ, and d) b-tagging event discriminant D_{Btag} for data and MC events after preselection. Contributions from $\mathrm{e^+e^-q\bar{q}}$, $\mathrm{q\bar{q}}$ and other backgrounds, dominated by $\mathrm{W^+W^-}$ production, are given separately. The distributions for expected signal events of $\tilde{\mathrm{t}}_{\mathrm{R}} \rightarrow \mathrm{c}\tilde{\chi}^0_1$ with $M_{\tilde{\mathrm{t}}_{\mathrm{R}}}$=90 GeV, $M_{\tilde{\chi}^0_1}$=60 GeV (a,b), $\tilde{\mathrm{t}}_{\mathrm{R}} \rightarrow \mathrm{b}\ell\tilde{\nu}$ with $M_{\tilde{\mathrm{t}}_{\mathrm{R}}}$=90 GeV, $M_{\tilde{\nu}}$=70 GeV (c) and $\tilde{\mathrm{b}}_{\mathrm{R}} \rightarrow \mathrm{b}\tilde{\chi}^0_1$ with $M_{\tilde{\mathrm{t}}_{\mathrm{R}}}$=90 GeV, $M_{\tilde{\chi}^0_1}$=60 GeV (d) are also shown.

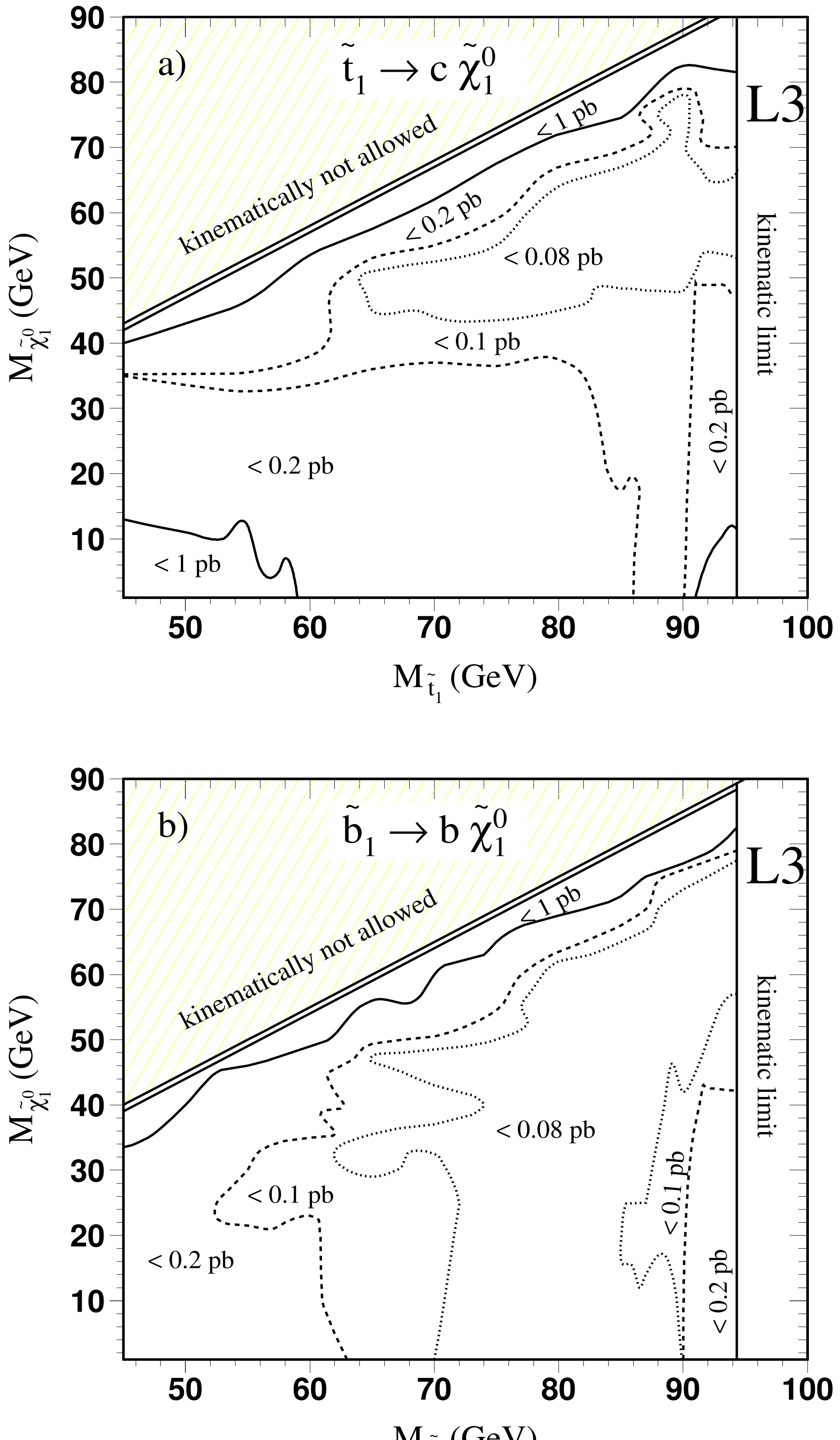

Figure 2: Upper limits on a) $e^+e^- \to \tilde{t}_1\bar{\tilde{t}}_1 \to c\tilde{\chi}^0_1\bar{c}\tilde{\chi}^0_1$ and b) $e^+e^- \to \tilde{b}_1\bar{\tilde{b}}_1 \to b\tilde{\chi}^0_1\bar{b}\tilde{\chi}^0_1$ production cross section times branching ratio. Limits are obtained by combining the results at centre of mass energies of $\sqrt{s}$=161–172 GeV, 183 GeV and 189 GeV.

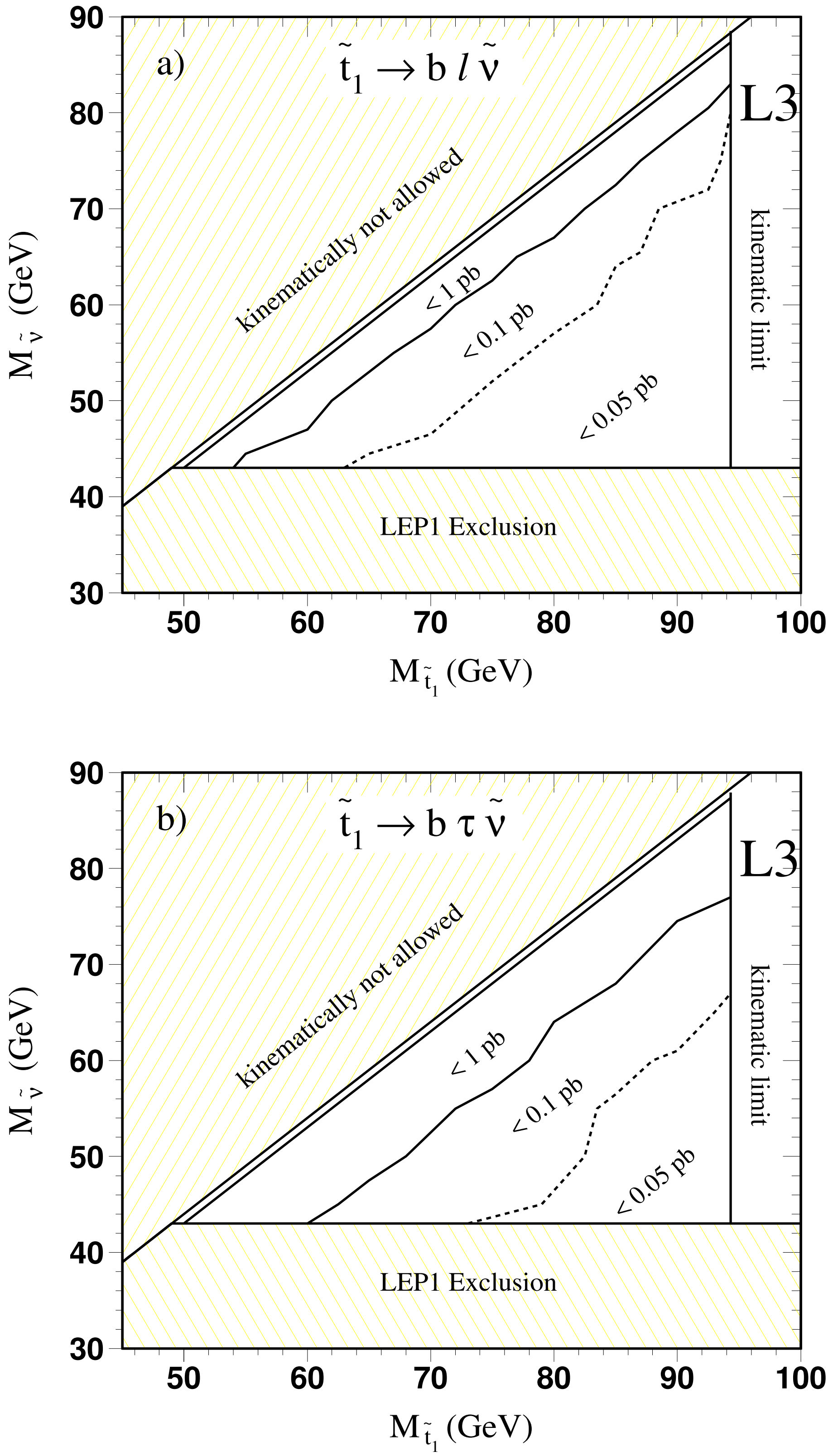

Figure 3: Upper limits on a) $e^+e^- \rightarrow \tilde{t}_1\bar{\tilde{t}}_1 \rightarrow b\ell^+\tilde{\nu}\bar{b}\ell^-\tilde{\nu}$, $\ell = e, \mu, \tau$ assuming lepton universality and b) $e^+e^- \rightarrow \tilde{t}_1\bar{\tilde{t}}_1 \rightarrow b\tau^+\tilde{\nu}\bar{b}\tau^-\tilde{\nu}$ production cross section times branching ratio. Limits are obtained from the $\sqrt{s}$=189 GeV data.

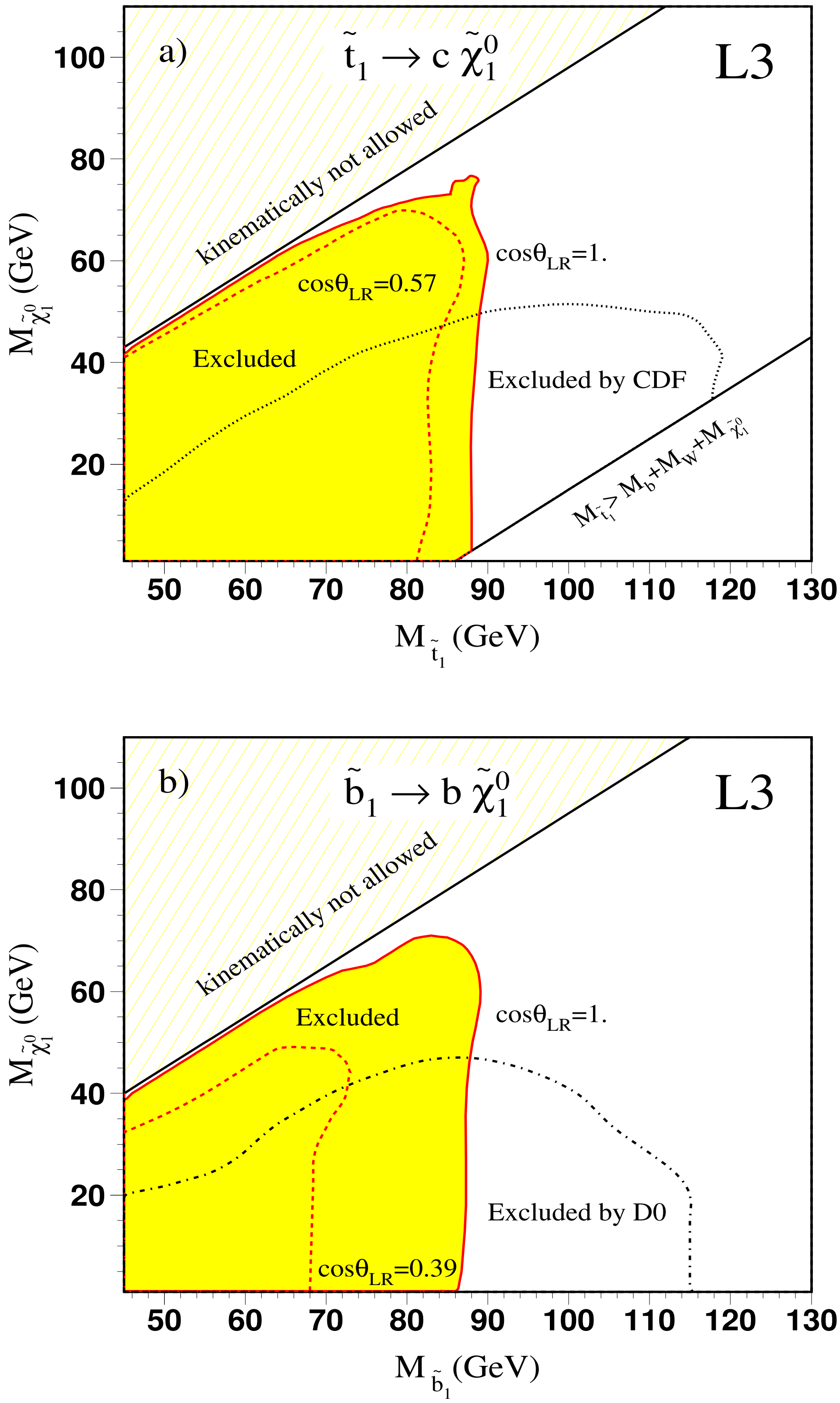

Figure 4: 95% C.L. exclusion limits in the MSSM on the masses of a) stop decaying via $\tilde{t}_1 \rightarrow c\tilde{\chi}^0_1$ and b) sbottom decaying via $\tilde{b}_1 \rightarrow b\tilde{\chi}^0_1$ as a function of the neutralino mass with maximal and minimal cross section assumptions. For comparison results on stop searches obtained by CDF [7] and on sbottom searches obtained by D0 [8] experiments are also shown.

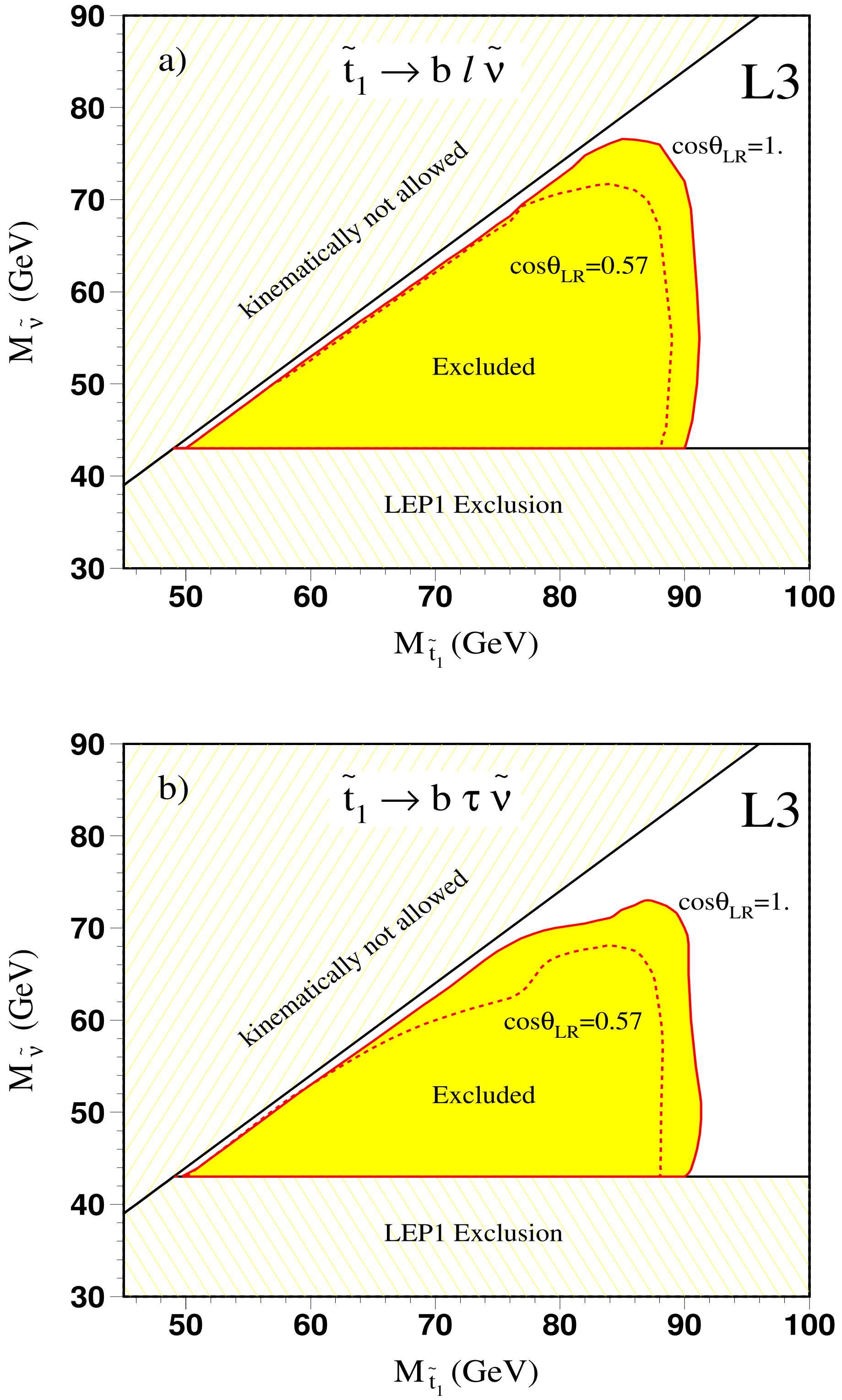

Figure 5: 95% C.L. exclusion limits in the MSSM on the mass of stop decaying via a) $\tilde{t}_1 \rightarrow b\ell\tilde{\nu}$, $\ell = e, \mu, \tau$ with equal probability and b) $\tilde{t}_1 \rightarrow b\tau\tilde{\nu}$, as a function of the sneutrino mass with maximal and minimal cross section assumptions. The sneutrino mass limit obtained at LEP1 is also shown.

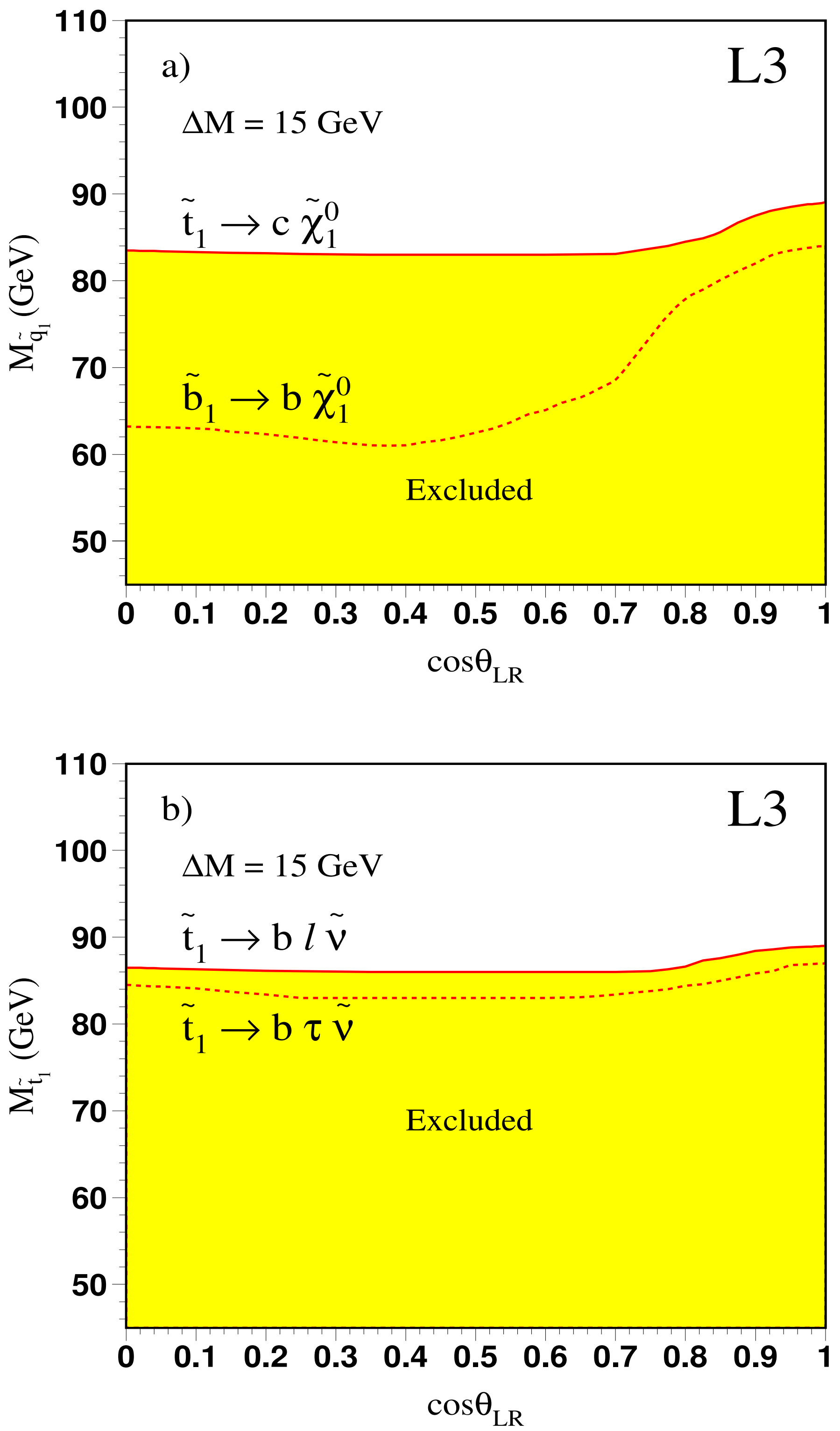

Figure 6: 95% C.L. exclusion limits in the MSSM as a function of the mixing angle $\cos\theta_{\mathrm{LR}}$ for the a) stop decaying via $\tilde{\mathrm{t}}_1 \rightarrow \mathrm{c}\tilde{\chi}^0_1$ (solid line) and sbottom decaying via $\tilde{\mathrm{b}}_1 \rightarrow \mathrm{b}\tilde{\chi}^0_1$ (dashed line), b) stop decaying via $\tilde{\mathrm{t}}_1 \rightarrow \mathrm{b}\ell\tilde{\nu}$, $\ell = e, \mu, \tau$ with equal probability (solid line) and $\tilde{\mathrm{t}}_1 \rightarrow \mathrm{b}\tau\tilde{\nu}$ (dashed line).

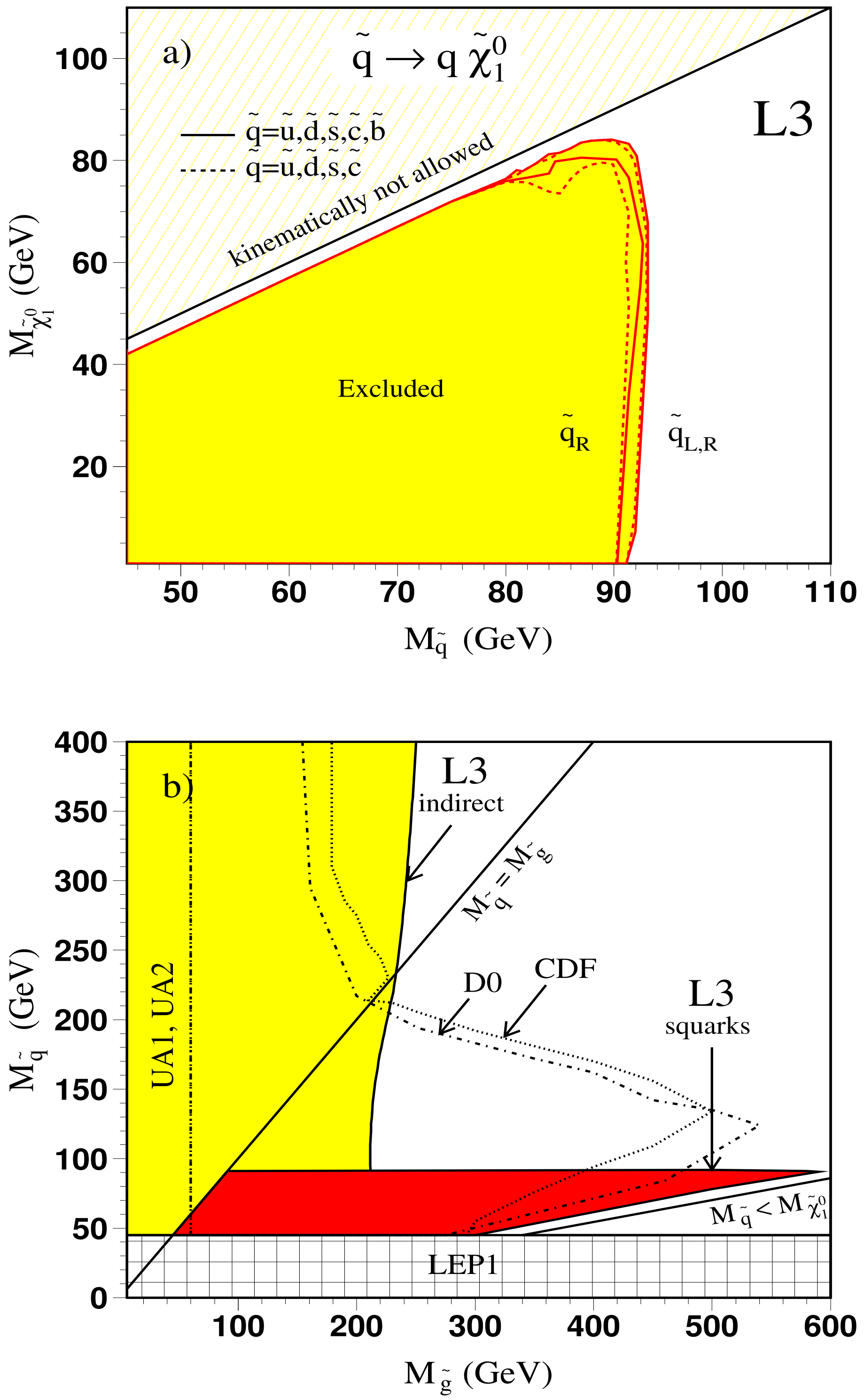

Figure 7: a) 95% C.L. exclusion limits in the MSSM on the masses of the degenerate squarks decaying via $\tilde{q} \rightarrow q\tilde{\chi}^0_1$. b) Excluded regions in the ($M_{\tilde{g}}$, $M_{\tilde{q}}$) plane. The dark shaded area is excluded from the search of squarks of the first two families, assuming the mass degeneracy among different flavours and between "left" - "right" squarks. The light shaded area illustrates indirect limits on the gluino mass, derived from the chargino, neutralino and scalar lepton searches. The regions excluded by the CDF and D0 collaborations [28] are valid for $\tan\beta = 4$ and $\mu = -400$ GeV. The exclusions obtained by the UA1 and UA2 [29] collaborations are also shown.